



COVER SHEET

This is the author version of article published as:

Steck, Roland and Knothe Tate, Melissa L. (2005) In silico stochastic network models that emulate the molecular sieving characteristics of bone. *Annals of Biomedical Engineering* 33(1):pp. 87-94.

Copyright 2005 Springer

Accessed from <http://eprints.qut.edu.au>

***In Silico* Stochastic Network Models that Emulate the Molecular Sieving Characteristics of Bone**

R. Steck¹, M. L. Knothe Tate^{1,2}

¹Orthopaedic Research Center, Lerner Research Institute, The Cleveland Clinic Foundation, Cleveland, USA

²Departments of Biomedical Engineering and Mechanical & Aerospace Engineering, Case School of Engineering, Case Western Reserve University, Cleveland, USA

Running headline: Bone Network Models with Molecular Sieving Character

Address for Correspondence:

Melissa L. Knothe Tate, PhD
Depts. of BME and MAE
Case Western Reserve University
10900 Euclid Ave.
Olin 219
Cleveland, OH 44106

Tel.: (216) 368 5884
Fax: (216) 368 4969
Email: knothetate@case.edu

ABSTRACT

Recent studies implicate bone's extracellular matrix as a "living electrophoresis and ion exchange column" with low pass filter function at the matrix level; whereas small molecules pass through the matrix microporosity, larger molecules penetrate the tissue through the pericellular space. In this study, stochastic network modeling principles were applied, for the first time to our knowledge, to build in silico, nano- to microscale models of bone. Small volumes of bone were modeled to include hierarchical levels of porosity comprising the bone matrix microporosity and the pericellular network. Flow and transport through the network was calculated for molecules from 1,000 to 100,000 Daltons. Based on this study, two contrasting effects determine the rate and direction of transport of different size molecules through the hierarchical porous network of bone. Whereas diffusivity of a given molecule decreases with increasing molecular size, size exclusion effects of bone's low pass molecular sieve translate into increasing flow velocities for large molecular species along transport paths located in the immediate vicinity of the cells. Both phenomena are expected to have a profound effect on the formation of molecular gradients at a tissue level, providing cues for tissue generation and repair by cellular "micromachines", e.g. osteoclasts and osteoblasts.

Keywords: Computational model, lacunocanalicular network, bone matrix microporosity, interstitial fluid flow, molecular transport

NOTATION

α_i	effective molecular radius of solute A, m
Δc_i	normalized concentration difference, -
C_i, C_j	concentration of a solute at the nodes i and j , kg m^{-3}
d	pore diameter, m
D_{mf}	free molecular diffusion coefficient, $\text{m}^2 \text{s}^{-1}$
D_P	pore diffusion coefficient for solute A through network, $\text{m}^2 \text{s}^{-1}$
ε_P	network porosity, -
J_{DA}	diffusion rate of solute A in a pore, kg s^{-1}
$K_A D_A$	effective diffusion coefficient, $\text{m}^2 \text{s}^{-1}$
l_p	pore length, m
μ	fluid viscosity, $\text{kg m}^{-1} \text{s}^{-1}$
MW	molecular weight, Daltons (Da)
N_{DA}	mass flux of solute A through pore, kg s^{-1}
Q_{ij}	volume flow rate through pore, $\text{m}^3 \text{s}^{-1}$
P	permeability of solute A through pore, $\text{m}^2 \text{s}^{-1}$
Δp_{ij}	pressure gradient across pore between nodes i and j , N m^{-3}
p_i, p_j	pressure at nodes i and j , N m^{-2}
R_P	characteristic distance of network, m
r_p	pore radius, m
r_s	Stokes radius for a molecule, m
r_g	radius of gyration for a molecule, m
v_{DA}	diffusion velocity of solute A, m s^{-1}
v_P	flow velocity through porous medium, m s^{-1}

INTRODUCTION

At an organ level, bone provides more surface area for ion exchange, protein elution and filtration of solutes than any other organ in the body.^{5,23,26} Within the interconnected porous network of bone, gradients of chemokines, cytokines, growth factors and other biomolecules not only influence but also provide a means to assess the physiological state of a cell at a local level. Furthermore, these molecular gradients provide cues for tissue generation and repair, *e.g.* osteoclastic resorption and subsequent osteoblastic apposition. The transport of paracrine and endocrine factors through bone tissue is poorly understood. The concentration of a given molecule depends on the size of that molecule and its binding sites, conformation, as well as diffusive and convective flow effects that influence the local (cellular) and global (tissue) dwell time of a given molecule within the system.^{5,6,9,10} Due to the interplay between bone's mechanical function and the formation of these time and location dependent chemical gradients, current theory of bone adaptation has shifted. Whereas previous adaptation theories emphasized direct transfer of mechanical signals from the systems level, through the organ and tissue levels, to the cells that have the machinery to remodel, current theory accounts for redundant mechanisms of transduction, *e.g.* mechanical modulated transport of bio-chemo-electrical signals that direct cellular level remodeling activity, as reviewed recently in Knothe Tate (2003)⁶ and Knothe Tate and Knothe (2000).⁷

Recent studies implicate bone's extracellular matrix as a "living electrophoresis and ion exchange column" with low pass filter function at the matrix level.^{5,11,26} Based on *in vivo* permeability studies, it has been shown that the hierarchical degrees of porosity in the bone matrix act as a molecular sieve for different sized solutes being transported through bone. Hence, molecules such as glucose and smaller amino acids (300-400 Daltons, Da) are expected to penetrate the matrix microporosity as well as the

pericellular network of the lacunocanalicular system.²⁶ Larger molecules such as cytokines, androgens and estrogens as well as serum derived proteins would not be expected to penetrate the matrix but may penetrate the pericellular space, in particular when driven by load-induced fluid flow or other convective effects. In addition to tracer transport studies demonstrating these effects,^{9,10,26} recent proton nuclear magnetic resonance spectroscopy (NMR) experiments show that fluid is transported within the matrix microporosity, albeit at very low diffusion rates.² As a consequence of these characteristics it is expected that a baseline supply of low molecular weight nutrients to the osteocytes is guaranteed under most circumstances, whereas the transport of hormones and other signaling molecules to- and from the osteocytes is more sensitive to the state of the pericellular network. In addition, the supply of these larger molecules to the osteocytes is also expected to be more susceptible to the enhancement of the transport capacity, *e.g.* by means of convective transport mechanisms.⁸

Studying molecular transport through the different levels of porosity is challenging due to the practical difficulties of viewing transport through the dense tissue of bone. Furthermore, the cellular network, referred to as osteocyte syncytium, changes depending on the physiological state of the tissue; *e.g.* measures including osteocyte density, connectivity and the canalicular tortuosity, change as a result of aging^{20,27} as well as disease or pathology.¹¹ These cellular level changes are expected to influence greatly both the paths as well as the rates of molecular transport through bone tissue. Characterization of the relationship between cellular organization and molecular transport in healthy and diseased bone would provide a basis to optimize design of delivery vehicles for exogenous and endogenous bioactive molecules and drugs across the tissue. The optimal delivery of pharmaceutical and bioactive agents is dependent on the location and time course of their application; this, in turn, depends on the diffusion

constant of the agent in the tissue, which is a function of the agent's molecular size. By using transport characteristics through healthy and diseased tissue as a design criteria for optimization of delivery vehicle design, many parallels may be drawn to the analogous process of *in vitro* molecular sieving for protein purification using chromatography columns .

Mathematical models have been developed to improve the throughput and selectivity of column chromatography. Some of the most commonly used models are the stochastic network models,¹³ which are based on the percolation theory. In these models, the different hierarchical levels of pores in a chromatography column are simulated by different classes of pores that penetrate the matrix and connect a system of nodes. Based on the solution for nodal parameters, such as fluid pressure or molecular concentration, global modal parameters, such as tissue permeability or diffusivity of a given molecule, can be determined. Stochastic network models have been applied to study transport through biological tissues,^{24,28} but to our knowledge these methods have not been applied previously to study the time and location dependent molecular sieving characteristics of bone.

The purpose of this study was to model bone as a hierarchical network of interconnected pores and to use network modeling methods to study transport of molecules through this highly controlled, idealized model. The ultimate goal of the model is to examine the development of chemical gradients in bone and to relate gradients of specifically sized molecules to those that are known to play a role in modulating cell activity in bone remodeling. As a first step in this process, we applied stochastic network modeling principles to build *in silico*, nano- to microscale models that emulate the molecular sieving characteristics of bone. For the purposes of this model, emphasis was placed on molecular sieving characteristics of the pericellular

transport pathways comprising the lacunocanalicular system and matrix microporosity, which constitute the “low pass” filter function of the bone matrix.²⁶

METHODS

A model was built to replicate pore size, number, and distribution of the porous network in bone (Fig. 1). The stochastic network simulations involved three steps. In the first step, the network was constructed using random and semi-random algorithms. In the second step, the network was reduced, according to the molecular size of the different tracers, to account for size exclusion effects in the simulation of molecular transport through the network. Finally, through the calculation of nodal parameters, the global tissue parameters for the network could be determined. Due to the stochastic nature of the network generation, the calculations were repeated for 20 different networks and average values were calculated. The simulations were programmed in Mathematica® (v. 4.0, Wolfram Research Inc., Champaign, IL) on a PC workstation. In the following, the individual steps are explained in more detail:

Network construction

First, we constructed a regular cubic lattice network with the dimension 15x15x15 nodes to represent a small volume (approx. $80^3 \mu\text{m}^3$) of cortical bone tissue (Fig. 2). Thereby each of the nodes was connected to its immediately neighboring six nodes via a pore. In order to model the bone matrix microporosity, two classes of pore sizes were assigned to these connecting pores, representing the spaces between collagen fibers, and the gaps between the apatite crystals and the collagen fibers, respectively. The two pore diameters were assigned randomly with a binomial distribution function. In addition, the two pore diameters per se were distributed normally around mean pore diameters (5.0

and 10.0 nm diameter, with a standard deviation of 1.0 nm for both pore sizes) to reflect the variability of the micropore size. In our models, the lengths of all micropores were equivalent to the distance between two nodes of the network, which is defined by the length of a side of the network cube divided by the number of nodes (in our case 15).

Next, the overlying (*i.e.* one hierarchical order above the matrix microporosity) lacunocanalicular network was constructed. The primary transport direction, the direction of the pressure or concentration gradient, was from the top to the bottom of the model cube, which is equivalent to the radial direction in an osteon. To ensure connectivity between the top and bottom plane, and to reflect the anisotropic nature of the lacunocanalicular network in Haversian bone with a preferred radial orientation of the canaliculi, this system was constructed through the formation of so-called percolation clusters. These connected the top with the bottom plane through number of nodes that were semi-randomly assigned as lacunae and were loosely aligned parallel to the general flow direction. The total number of lacunae was thereby consistent with the average osteocyte density in human cortical bone²⁷. These nodes were interconnected by large-diameter canaliculi (160 nm), primarily in the flow direction, but also amongst different percolation clusters, provided that the distance between two given lacunae was smaller than a certain threshold value (Fig. 2). It should be noted that the entire pore volume of the network was made up of the connecting pores, and the nodes were assumed to have no volume.

Flow and transport through the model was calculated between the top and bottom plane of the network, in the $-z$ direction. To ensure continuity in x and y direction, periodic boundary conditions were implemented and the nodes at $x=L$ and $y=L$ were connected to the nodes at $x=0$ and $y=0$.

Network reduction

Flow and diffusive transport of dextrans with molecular weights (MW) between 1,000 and 100,000 Daltons (Da) was calculated through the network. The effective molecule size was compared to the pore diameters of the model. For dextrans, two different methods are reported in the literature for calculating the effective molecule size from the molecular weight. The Stokes' radius r_s (in nm) for a dextran molecule of known molecular weight has been determined to be ¹⁸

$$r_s = 0.0488 \cdot MW^{0.437} \quad (1)$$

Alternatively, for long flexible chains, such as dextran molecules, the radius of gyration r_g can be used ¹⁹.

$$r_g = 0.0323 \cdot \sqrt{MW} \quad (2)$$

We then compared the radii calculated with these two methods (Fig. 3). They are similar only for very small MW (ca. 1,000 Da). For increasing MW the radius of gyration is always bigger, by more than 25% at 20,000 Da and by more than 35% at 100,000 Da. Both values were calculated for the simulated molecules and compared with the pore diameters. Pores that are not accessible, because they are too narrow to allow passage of a given sized molecule, were excluded from the network. A side effect of removing these pores was the formation of so-called “dead end” pores, as well as of isolated nodes that did not contribute to the flow or diffusion through the model; hence, they were also excluded from the network.

Parameter calculation

All calculations were based on the methods described in Meyers and Liapis, 1998.¹³ The goal of the calculations was to determine nodal parameters by solving a system of linear algebraic equations, in order to calculate global model parameters.

Flow calculations

The flow rate Q_{ij} through a cylindrical pore between the two nodes i and j with a pressure gradient Δp_{ij} can be approximated using the equation (3), under the assumption of creeping flow conditions (low Reynolds number).

$$Q_{ij} = \frac{(p_i - p_j)d^3}{\left(\left(\frac{128l_p}{\pi d} + 24 \right) \mu \right)} \quad (3)$$

where l_p and d are the pore length and diameter, and μ is the dynamic fluid viscosity. This equation was set up for every pore of the network. In addition, there was conservation of mass at the nodes, so the sum of the flow rates in all the pores connecting the node with its neighbors had to be zero. This equilibrium equation could be set up for every node. In combination, this led to a system of linear equations that could be solved numerically for the fluid pressures at all nodes. A static pressure gradient of 100 kPa/mm, which is comparable to the fluid pressure gradient in mechanically loaded bone, calculated using poroelastic finite element models, was applied across the network and served as boundary condition for these simulations.

The total flow rate across the network could now be calculated by adding up the flow rates through all the pores that cross any x - y plane of the network. This led to the average fluid velocity, which is calculated by dividing the total flow rate by the sum of the cross sectional area of all pores in this plane.

Diffusive transport

Diffusive transport, driven by a concentration gradient across the network, was calculated for different size dextran molecules. If a linear concentration gradient ΔC_A can be assumed, and adsorption can be excluded, the diffusion rate J_{DA} of the molecules of a species A through pores of the length l_p and radius r_p can be calculated as follows

$$J_{DA} = \pi r_p^2 K_A D_A \left(\frac{\Delta C_A}{l_p} \right) \quad (4)$$

where the effective diffusivity $K_A D_A$ is given by

$$K_A D_A = D_{mf} \left(1 - \frac{\alpha_1}{r_p} \right)^2 \left[1 - 2.104 \left(\frac{\alpha_1}{r_p} \right) + 2.09 \left(\frac{\alpha_1}{r_p} \right)^3 - 0.95 \left(\frac{\alpha_1}{r_p} \right)^5 \right] \quad (5)$$

D_{mf} is the free molecular diffusion coefficient for molecules of the species A and α_1 is its effective molecular radius. In equation (5), the restricting effects of steric hindrance (second term) and frictional resistance (third term) on the diffusion are taken into account. Using the above equations, the mass flux $N_{DA,ij}$ of the molecules of a species A through pores of the length l_p can be determined with the following formula

$$N_{DA,ij} = (K_A D_A)_{ij} \left(\frac{C_i - C_j}{l_{p,ij}} \right) \quad (6)$$

Similarly to the flow calculations, the net volume flux at each node must be zero. This leads to a system of algebraic equations that can be solved for the molecular concentration at each of the nodes of the network.

Based on the known nodal concentrations, the total permeability P of the network for molecules of the species A can be calculated from equation (7):

$$P = \left(\frac{1}{2} \right) \left(\frac{1}{S_0} \right) \left[\sum_{i=1}^{N_A} \sum_{j=1}^{N_A} \pi (r_{p,ij})^2 (K_A D_A)_{ij} \left(\frac{\Delta C_{ij}}{v_{ij}} \right) \right] \quad (7)$$

where N_A is the total number of nodes in the network and v_{ij} represents the ratio of the pore length $l_{p,ij}$ to the distance between node i and its nearest neighbor. It is important to note that the permeability calculated with this formula is defined in Meyer and Liapis, 1998¹³ in a chemical engineering context, where P has the unit of a diffusion constant (m^2s^{-1}). The other terms in the equation are S_0 , which represent the cross sectional area of the model cube and Δc_{ij} , the normalized concentration difference, where

$$c_i = \frac{(C_i - C_{N_e})}{(C_1 - C_{N_e})}; \quad C_1 = 1; \quad C_N = 0 \quad (8)$$

Since it is only the pores in the z direction that contribute to the net flux through the network, only these pores were taken into account in equation (8). Finally, this led to the equation for the pore diffusion coefficient for molecules of a species A through the network

$$D_p = \frac{P}{\varepsilon_p} \quad (9)$$

where ε_p is the network porosity.

Fluid velocity vs. diffusion velocity

To examine the effect of a pressure gradient on the transport capacity across a porous network, we calculated the ratio between the velocity of the permeating fluid v_p versus the diffusion velocity v_{DA} . The diffusion velocity v_{DA} of the molecules of a species A can be calculated from D_p/R_p (D_p is the diffusion coefficient and R_p represents a characteristic distance of the network, in our case the width of the model cube L)

RESULTS

For both methods used to calculate the effective molecular size, the average pore connectivity decreased from 7.44 ± 0.05 (average \pm standard deviation) at a molecular

weight of 1,000 Da to 1.47 ± 0.05 at 100,000 Da. This resulted in an increase in pressure driven transport velocity through the network for increasing molecular weight (Fig. 4), whereby a higher flow velocity (by approx. 5 %) and a more prominent increase in flow velocity, for molecular weights between 5,000 and 10,000 Da, was observed in the model where radius of gyration was used to define effective molecule size. In contrast, the effective pore diffusion coefficient, or diffusivity, decreased exponentially (Fig. 5) with increasing molecular weight. For molecules of 1,000 Da, the diffusivity was 40% less if one calculates the molecular size based on the radius of gyration compared to that based on the Stokes' radius. For higher molecular weight molecules up to 100,000 Da, the difference in the calculated diffusion constant was only 10%.

Finally, the ratio between the pressure-driven fluid velocity and the diffusion velocity through the network increased almost linearly with increasing molecular weight (Fig. 6). For the model using the radius of gyration, the ratio increases from almost $4.3 \cdot 10^4$ for 1,000 Da to more than $2.5 \cdot 10^6$ for 100,000 Da, whereas the ratios for the model using the Stokes radius were consistently about 50% smaller, but showed the same tendency.

DISCUSSION

Stochastic network modeling principles were applied to build *in silico*, nano- to microscale models that emulate the molecular sieving characteristics of bone. Two contrasting effects determine the rate and direction of transport of large molecules through the hierarchical porous network of the *in silico* bone model. Whereas the molecular weight is the main determinant of diffusive transport rate through a homogenous network, size exclusion and flow velocity effects play an important role for transport through a network exhibiting some of the complexities inherent to bone

including the hierarchical porosity and convective effects of load-induced fluid flow. Based on calculations of the pressure driven flow velocities for different size molecules across the network, it was shown that flow velocity increased with increasing molecular weight of the transported molecules. This is due to the shorter effective transport pathways available for transport of the larger molecules, analogous to more rapid transport of larger proteins due to size exclusion in chromatography columns. Since the pressure gradient across the cube remains constant and the mean transport distance shortens, transport velocities increase with larger molecules. In contrast, the diffusivity for higher molecular weight substances decreases rapidly with increasing molecular weight, due to the combined effects of steric hindrance at the entrance to each pore and frictional restriction within each pore. Taken as a whole, the relationship between contrasting effects of the increased flow velocity and reduced diffusivity with increasing molecular weight underscore the importance of convective transport mechanisms for the distribution of higher molecular weight substances in tissues such as bone.

The average connectivity of a stochastic network, comprising the average number of pores connecting a node with its neighbors, is a key parameter for the determination of the transport properties of a porous medium.¹³ The maximal average connectivity is equal to the lattice coordination number, which is six in a regular cubic lattice. When pores are removed from the network, the connectivity decreases. If it falls below a certain percolation threshold, the connection between two sides of the network, referred to as a percolation cluster, is no longer guaranteed, and transport across the network ceases. For a regular cubic lattice, the percolation threshold is typically 2.488.²⁵ However, since our networks consist of an underlying regular cubic lattice with additional canalicular pores, the maximal connectivity for the network is 7.44 ± 0.05 (average \pm standard deviation), *i.e.* higher than six. Furthermore, because these

additional pores have been created in a semi-random process, transport across the network is still guaranteed for values of the pore connectivity comprising 1.47 ± 0.05 .

We employed two different methods to calculate the effective size of the dextran molecules of different molecular weights (equations 1 and 2). Both methods have been developed for simulations of the glomerular filtration of dextran molecules.^{18,19} The first method uses the Stokes radius as the effective molecule size. It has been reported that the Stokes radius is well suited to characterize globular molecules, but may be less suited to characterize long, flexible chain molecules such as dextrans and polymers. Therefore, models that were based on the radius of gyration, (the second method), have been more successful in predicting transport rates of dextran in other biological tissues.¹⁹ The radius of gyration for a dextran molecule is larger than its Stokes radius (Fig. 3), which implies that the long chain molecules exhibit a higher resistance for transport through narrow pores than globular molecules of the same molecular weight. In contrast, experimental tracer studies in bone have shown that dextran molecules do penetrate through narrow pores, *e.g.* when the molecule aligns along the pore orientation; this phenomenon has been described as microextrusion.²⁶ Eventually, systematic and quantitative validation studies, *in vivo* or *ex vivo*, will have to be performed to determine which of the two methods is more appropriate for use in studies of transport of dextran molecules through bone tissue. For the current feasibility study, the molecular sieving characteristics of bone could be demonstrated successfully using both methods.

This study represents a first application of stochastic network modeling techniques to bone with the primary objective to demonstrate the feasibility and power of this method. In this early stage of development, the model exhibits certain limitations, which will be addressed in future evolutions of the model. For instance, the flow

through the pores was simulated as basic pipe flow, and the pore geometry was assumed to be cylindrical. In reality, the canaliculi in bone are partly filled with the osteocyte processes, so that there is actually annular flow between the osteocyte process and the canalicular wall. Furthermore, this space is not empty or simply fluid filled but constitutes a small territory around the cell that has not completely mineralized; hence, the space is likely to be filled with a network of matrix molecules such as glycosaminoglycans that may interact with plasma membrane proteins on the cell surface, which would alter the flow characteristics. Flow through this matrix would be comparable to that through an electrophoresis gel; therefore, this pericellular matrix is likely to exhibit molecular sieving properties as well.²⁶ The bone matrix microporosity was simulated by two classes of pores with mean pore diameters of 5 and 10 nm. There is little information in the literature about the distribution and structure of the pores in the bone matrix. They have been described to be generally on the order of 10 nm diameter,¹ and more specifically, the pores between the apatite crystals have been measured to be between 10 and 25 nm in diameter, with some pores up to 50 nm in diameter.³ More importantly, it is not known what portion of the fluid trapped in these pores is actually mobile. While some studies indicate that the interstitial fluid is chemically bound,^{16,17} other experiments have demonstrated that low molecular weight tracers (~300 Da) are able to penetrate the matrix,²⁶ which would suggest that at least some of the fluid is exchanged between the matrix micropores and the macropores of the lacunocanalicular system; this has been corroborated recently using NMR.² Hence, although the pores of the bone matrix have been measured to be greater than the 5 to 10 nm used in this model, we have chosen these values as an effective pore size range based on our experience from the tracer experiments.

Interstitial fluid flow through the lacunocanalicular system and the bone matrix

microporosity was calculated as a result of a pressure gradient, which is induced, in vivo or in vitro, by mechanical loading of the poroelastic bone. Although this pressure gradient is time dependent in vivo, we have used a static pressure gradient in this model with the justification that we are examining at a short time period during a load cycle, for which the pressure gradient can be assumed constant. Quantitatively, the calculated flow velocities in our model are highly dependent on the choice of this pressure gradient. Unfortunately, very few actual measurements of interstitial fluid pressure gradients have been reported in the literature. Qin et al.²¹ have measured the fluid pressure in the medullary canal of turkey ulnas subjected to near physiological compression and bending loads. Their results, averaged over the width of the entire cortex, lead to a pressure gradient of approximately 6 kPa mm^{-1} . The same group has developed computational models in parallel to their experimental models, where they predicted local intracortical pressure gradient peaks of up to 360 kPa mm^{-1} at a physiological loading frequency of 1 Hz .²² We chose a pressure gradient of 100 kPa mm^{-1} in our model, which lies in between these measured average and predicted peak pressure gradients. In a sensitivity analysis of our network model we found that the calculated fluid velocities are directly proportional to the pressure gradient applied across the network.

Neighboring osteocytes in bone are interconnected by canaliculi. The number of connecting canaliculi between two osteocytes depends on the proximity and the orientation of the osteocytes. Osteocytes that are close to each other and lie approximately in the same transverse plane (with respect to the longitudinal axis of the bone), are connected by several canaliculi, whereas osteocytes that are further apart and in different longitudinal positions are connected by a smaller number of canaliculi. Few studies have reported systematic and quantitative analyses of these relationships.^{4,12,14}

Hence, given the lack of quantitative reference data, and for model idealizations, neighboring osteocytes are connected by single canaliculi in the current model, independent of distance and orientation. As part of an ongoing effort to determine the critical state of osteocyte connectivity to insure intercellular communication through mechanochemical and –electrical signaling, evaluations are currently underway to quantify the number of canaliculi connecting two osteocytes in bone. The results of these studies, will be implemented in further stages of model development by either increasing the number of connecting canaliculi in the model, or by adjusting the flow rate between two osteocytes to take the increased transport through a higher number of canaliculi into account. The implementation of a single connecting canaliculus between osteocytes can partly explain the relatively low values for the transport parameters of dextran in bone, such as the diffusivity, that were calculated with this model. In the current model, emphasis was placed on simulating realistic osteocyte density for cortical bone as well as approximating the effective pore size ranges in cortical bone. Thus, the ratio of the volume of all the pores of the resulting network to the volume of the network cube is, with 0.012 percent currently well below the generally assumed porosity of cortical bone, which is reported to be on the order of five percent for the lacunocanalicular system.¹⁵ Thus, although the calculated transport parameters for our models demonstrate relative trends, it would not be appropriate to compare them numerically with experimentally measured values.

In conclusion, stochastic network modeling was applied for the first time to our knowledge to build an *in silico*, nano- to microscale model that emulates the molecular sieving characteristics of bone. This is a first step in modeling biophysical characteristics of bone that have been virtually ignored in the literature to date, including *e.g.* the incorporation of ion exchange, extra- and intracellular transport and of charge

interactions in the flow rate and transport equations. Based on this study, not only does convective transport augment transport of large molecular weight substances with relative low diffusivity, but size exclusion effects of the hierarchical bone pore network may also increase transport rates along specific transport paths in the immediate vicinity of the cells. Both of these biophysical phenomena are expected to have a profound effect on the formation of molecular gradients at a tissue level, providing cues for tissue generation and repair by cellular “micromachines”, *e.g.* osteoclasts and osteoblasts. In the future, these effects may be exploited to develop a new generation of pharmaceuticals, drug delivery vehicles or treatment strategies.

ACKNOWLEDGMENTS

This study was supported, in part, by a research grant from the AO Foundation, Switzerland (04-S4).

REFERENCES

1. Cowin, S. C. Bone poroelasticity. *J Biomech.* 32:217-238, 1999.
2. Fernandez-Seara, M. A., S. L. Wehrli and F. W. Wehrli. Diffusion of exchangeable water in cortical bone studied by nuclear magnetic resonance. *Biophys.J.* 82:522-529, 2002.
3. Holmes, J. M., D. H. Davies, W. J. Meath and R. A. Beebe. Gas Adsorption and Surface Structure of Bone Mineral. *Biochem.* 19:2019-24.:2019-2024, 1964.
4. Kamioka, H., T. Honjo and T. Takano-Yamamoto. A three-dimensional distribution of osteocyte processes revealed by the combination of confocal laser scanning microscopy and differential interference contrast microscopy. *Bone.* 28:145-149, 2001.

5. Knothe Tate, M. L. "Interstitial fluid flow." In: *Bone Mechanics Handbook*, edited by S. C. Cowin. CRC Press, 2001, pp. 1-29.
6. Knothe Tate, M. L. "Whither flows the fluid in bone?" An osteocyte's perspective. *J.Biomech.* 36:1409-1424, 2003.
7. Knothe Tate, M. L. and U. Knothe. An ex vivo model to study transport processes and fluid flow in loaded bone. *J Biomech.* 33:247-254, 2000.
8. Knothe Tate, M. L. and P. Niederer. Theoretical FE-based model developed to predict the relative contribution of convective and diffusive transport mechanisms for the maintenance of local equilibria within cortical bone. *Adv. Heat Mass Transf. Biotech. Trans. ASME.* 1998, 133-142 p.
9. Knothe Tate, M. L., P. Niederer and U. Knothe. In vivo Tracer Transport through the Lacunocanalicular System of Rat Bone in an Environment Devoid of Mechanical Loading. *Bone.* 2:107-117, 1998.
10. Knothe Tate, M. L., R. Steck, M. R. Forwood and P. Niederer. In vivo demonstration of load-induced fluid flow in the rat tibia and its potential implications for processes associated with functional adaptation. *J Exp. Biol.* 203:2737-2745, 2000.
11. Knothe Tate, M. L., A. E. Tami, T. W. Bauer and U. Knothe. Micropathoanatomy of Osteoporosis: Indications for a Cellular Basis of Bone Disease. *Adv. Osteopor. Frac. Man..* 2:9-14, 2002.
12. Marotti, G., M. Ferretti, M. A. Muglia, C. Palumbo and S. Palazzini. A quantitative evaluation of osteoblast-osteocyte relationships on growing endosteal surface of rabbit tibiae. *Bone.* 13:363-368, 1992.

13. Meyers, J. J. and A. I. Liapis. Network modeling of the intraparticle convection and diffusion of molecules in porous particles packed in a chromatographic column. *J. Chromat.* 827:197-213, 1998.
14. Mishra, S. and M. L. Knothe Tate. Effect of lacunocanalicular architecture on hydraulic conductance in bone tissue: Implications for bone health and evolution. *Anat.Rec.* 273A:752-762, 2003.
15. Morris, M. A., J. A. Lopez-Curto, S. P. Hughes, K. N. An, J. B. Bassingthwaite and P. J. Kelly. Fluid spaces in canine bone and marrow. *Microvasc.Res.* 23:188-200, 1982.
16. Neuman, W. F. and M. W. Neuman. *The Chemical Dynamics of Bone*. University of Chicago Press. 1958.
17. Neuman, W. F., T. Y. Toribara and B. J. Mulvan. The Surface Chemistry of Bone. VII The Hydration Shell. *J.Am.Chem.Soc.* 75:4239-4242, 1953.
18. Oliver, J. D., Iii, S. Anderson, J. L. Troy, B. M. Brenner and W. H. Deen. Determination of glomerular size-selectivity in the normal rat with Ficoll. *J. Am. Soc. Nephrol.* 3:214-228, 1992.
19. Oliver, J. D., Iii and W. M. Deen. Random-coil model for glomerular sieving of dextran. *Bull. Math. Biol.* 56:369-389, 1994.
20. Power, J., N. Loveridge, N. Rushton, M. Parker and J. Reeve. Osteocyte density in aging subjects is enhanced in bone adjacent to remodeling haversian systems. *Bone.* 30:859-865, 2002.
21. Qin, Y. X., T. Kaplan, A. Saldanha and C. Rubin. Fluid pressure gradients, arising from oscillations in intramedullary pressure, is correlated with the formation of bone and inhibition of intracortical porosity. *J.Biomech.* 36:1427-1437, 2003.

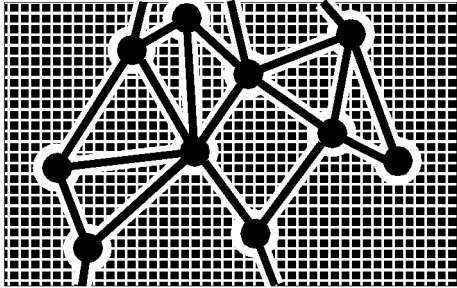
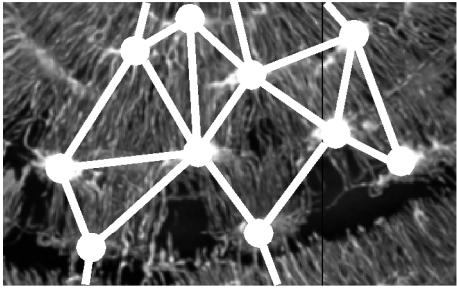
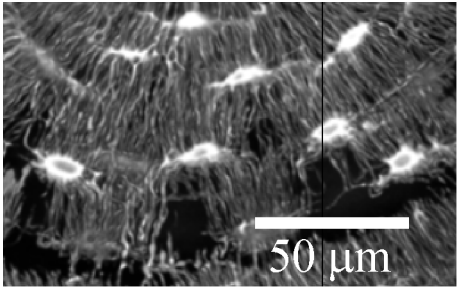
22. Qin, Y. X., K. J. Mcleod, M. W. Otter and C. T. Rubin. The interdependent role of loading frequency, intracortical fluid pressure and pressure gradients in guiding site-specific bone adaptation. *Trans. 44th Ann. Meet.*. 1998, 544 p.
23. Robinson, R. A. "Observations regarding compartments for tracer calcium in the body." In: *Bone Biodynamics*, edited by H. M. Frost. London: Churchill Publishers, 1964, pp. 423-439.
24. Saltzman, W. M. and R. Langer. Transport rates of proteins in porous materials with known microgeometry. *Biophys. J.* 55:163-171, 1989.
25. Stauffer, D. and A. Aharony. *Introduction to Percolation Theory*. Taylor & Francis Ltd. 1994.
26. Tami, A. E., M. B. Schaffler and M. L. Knothe Tate. Probing the tissue to subcellular level structure underlying bone's molecular sieving function. *Biorheol.* 40:577-590, 2003.
27. Vashishth, D., O. Verborgt, G. Divine, M. B. Schaffler and D. P. Fyhrie. Decline in osteocyte lacunar density in human cortical bone is associated with accumulation of microcracks with age. *Bone.* 26:375-380, 2000.
28. Yuan, F., A. Krol and S. Tong. Available space and extracellular transport of macromolecules: effects of pore size and connectedness. *Ann.Biomed.Eng.* 29:1150-1158, 2001.

FIGURE CAPTIONS

- Figure 1: Top: Reconstruction from confocal microscopy image stacks of human cortical bone samples, showing the lacunocanalicular network volume. Center: The osteocytes and their interconnections are highlighted. Bottom: Virtual, two-dimensional representation of the lacunocanalicular network and the bone matrix microporosity.
- Figure 2: Example of an actual network within a 15x15x15 node cube, with a side length of 80 μm , as simulated in this study. The osteocyte lacunae, displayed as dots, are connected by canaliculi. In this rendering, only one plane of the three-dimensional microporosity network is shown.
- Figure 3: Two methods for calculating the effective molecular size of the simulated dextran molecules have been used in the model. The radius of gyration (dashed line) for a molecule with a given molecular weight is predicted to be larger than the Stokes radius (continuous line). For comparison, the average radii of the two classes of matrix micropores are plotted as horizontal lines.
- Figure 4: The interstitial fluid velocity increases for molecules above a molecular weight of 7,000 Da and reaches a plateau at about 70,000 Da. The standard deviation for the fluid velocities averaged from 20 calculations for each molecular weight was 18 - 20%.

Figure 5: The diffusivity initially decreases exponentially with increasing molecular weight of the dextran molecules, for molecular weights of up to 10,000 Da. Above 10,000 Da, this decrease is much less pronounced and is almost linear. The standard deviation for the averaged diffusivities after 20 calculations was 75%

Figure 6: The ratio between interstitial fluid velocity and diffusion velocity of dextran through the network increases linearly with increasing molecular weight. This indicates that convection enhanced transport processes are particularly effective for high molecular weight substances.






-  Bone matrix microporosity
-  Osteocyte and lacuna
-  Osteocyte process and canaliculus

Figure 1

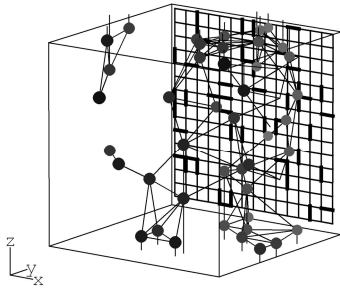


Figure 2

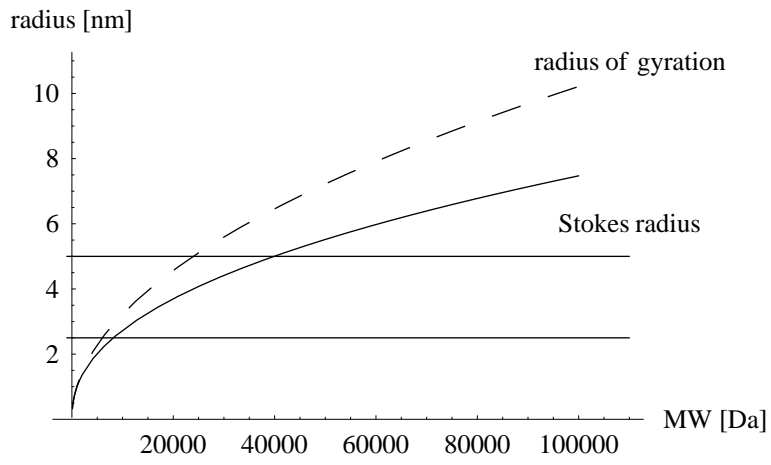


Figure 3

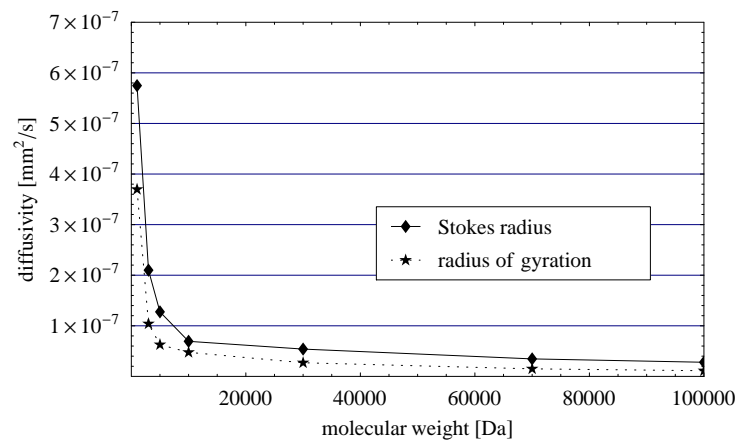


Figure 4

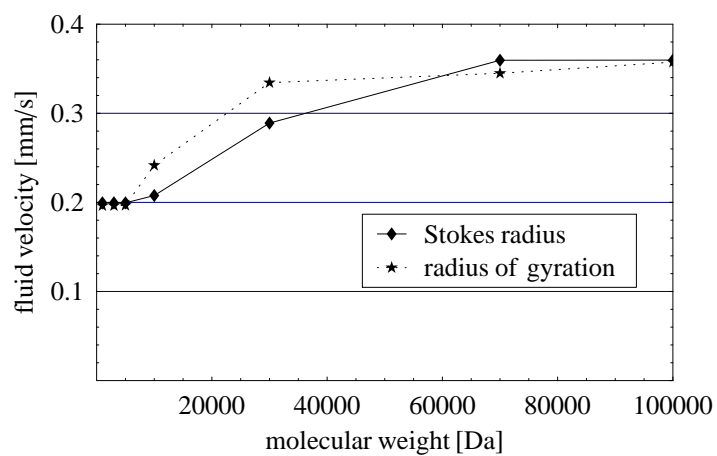


Figure 5

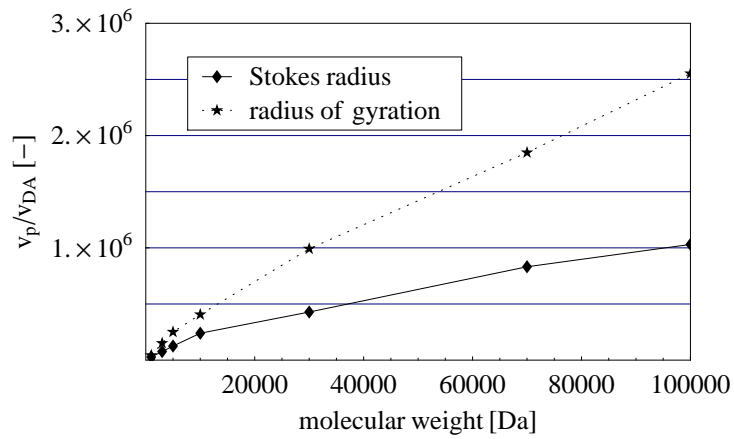


Figure 6